CHALMERS
UNIVERSITY OF TECHNOLOGY

Evaluation of Comsol Multiphysics for modelling of fluidized bed combustion

Master's thesis in Sustainable Energy Systems

ELISABETH CIMA

Department of Energy and Environment
CHALMERS UNIVERSITY OF TECHNOLOGY
Gothenburg, Sweden 2015

Evaluation of Comsol Multiphysics for modelling of fluidized bed combustion

ELISABETH CIMA

Department of Energy and Environment
Division of Energy Technology
CHALMERS UNIVERSITY OF TECHNOLOGY
Gothenburg, Sweden 2015

Evaluation of Comsol Multiphysics for modelling of fluidized bed combustion
ELISABETH CIMA

Supervisors: Robert Johansson, Department of Energy and Environment
             Tove Karlsson, Department of Energy and Environment

Examiner: Robert Johansson, Department of Energy and Environment

Department of Energy and Environment
Division of Energy Technology
Chalmers University of Technology
SE-412 96 Gothenburg
Telephone +46 31 772 1000

Evaluation of Comsol Multiphysics for modelling of fluidized bed combustion
ELISABETH CIMA
Department of Energy and Environment
Chalmers University of Technology

Abstract

Fluidized bed (FB) combustion offers an efficient and flexible way of producing heat and power from a large range of solid fuels. The installed capacity of FB boilers has increased steadily over the last years and there are today units as large as $460\,\mathrm{MW}_e$. The continued development and scale up of FB boilers require research, where an important tool that could assist the development is modelling of the combustion processes.

Due to the complex fluid dynamics and fuel conversion phenomena in FB boilers, comprehensive modelling of these units require simplified ways to describe the combustion process. In the present work, a model describing the mass and heat transfer in a bubbling fluidized bed (BFB) has been implemented in Comsol Multiphysics, version 5.1.

The aim of the work is to investigate the possibilities and challenges of using Comsol for modelling of FB boilers. Reasonable results are obtained for the mass balance whereas further work is required for the coupled mass and heat balance. It is concluded that Comsol offers a flexible environment for this type of modelling. However, the flexibility is also challenging, and more complex models require a solid knowledge about the software.

Acknowledgements

I want to thank Tove Karlsson and Robert Johansson. You have helped me and been a great support for me during the work.

I would like to thank Louise Lundberg for her interest in my work and for the help I received.

I also want to thank David Pallarès for making the work possible, for his interest in my work, and for lending me his computer.

Contents

List of figures

List of figures

List of tables

Acronyms

Acronym	Expansion
BBM	Black box models
BFB	Bubbling fluidized bed
CFB	Circulating fluidized bed
CFD	Computational fluid dynamics
CFDM	Computational fluid dynamics models
FB	Fluidized bed
FEM	Finite element method
FM	Fluidization models

Nomenclature

For variables which are not connected to a certain physical quantity the unit is marked with a star ($\star$).

Greek symbols

Symbol	Description	Unit
ϵ	Bed porosity	
λ	Heat conductivity	W·m^{-1}· K^{-1}
μ	Dynamic viscosity	Pa·s
ν	Stoichiometric coefficient	
Ω	Stoichiometric number of moles carbon per mole oxygen	
Φ	Arbitrary field variable	$\star$
ϕ	Flow potential	$\star$
ρ	Density	kg·m^{-3}

Roman symbols

Symbol	Description	Unit
A	Area	m^2
C	Molar concentration	mole·m^{-3}
C_p	Heat capacity	J·mole^{-1}·K^{-1}
D	Diffusion/dispersion coefficient	m^2· s^{-1}
d	Diameter	m
ΔH	Heat of reaction/phase transition	J·mole^{-1}
E_A	Activation energy	J·mole^{-1}
g	Gravitational constant	m·s^{-2}
H	Height	m
h_h	Heat transfer coefficient	W·m^{-2}·K^{-1}

h_m	Mass transfer coefficient	m·s^{-1}
k	Reaction rate constant	$\star$
K_{be}	Mass transfer coefficient	s^{-1}
$k_{r_{eff}}$	Effective rate constant of char conversion	m·s^{-1}
L	Characteristic length	m
M_c	Molar mass of carbon	kg·mole^{-1}
$\dot{N}$	Molar flux	mole·m^{-2}·s^{-1}
n_p	Number of char particles per furnace volume	m^{-3}
P	Pressure	Pa
$\dot{p}$	Rate of char particles	m^{-3}·s^{-1}
$\dot{Q}$	Heat flux	W·m^{-2}
$\dot{q}$	Heat source	W·m^{-3}
R	Ideal gas constant	J·mole^{-1}·K^{-1}
r	Reaction rate	mole·m^{-3}·s^{-1}
S	Source term	mole·m^{-3}·s^{-1}
T	Temperature	K
u	Velocity	m·s^{-1}
u_0	Primary air velocity at inlet	m·s^{-1}
$\vec{u}$	Velocity field	m·s^{-1}
V	Volume	m^3

Dimensionless numbers

Symbol	Name	Definition
Ar	The Archimedes number	$Ar = \dfrac{gL^3\rho(\rho_s - \rho)}{\mu^2}$
Re	The Reynolds number	$Re = \dfrac{\rho u L}{\mu}$
Sh	The Sherwood number	$Sh = \dfrac{h_m L}{D}$

Subscripts

Subscript	Description
b	Bubble phase
bm	Bed material
c	Char/carbon
k	Char class index
e	Emulsion phase
f	Fuel
g	Gas
i	Species index
∞	Bulk
j	Reaction
l	Layer
m	Moisture
mf	Minimum fluidization
n	Source index
p	Particle
s	Solids
v_i	Volatile specie
v	Volatiles
w	Wall

1

Introduction

On a global scale, the generation of heat and power accounts for more than 40% of the world energy consumption [1]. Of this share approximately 40% of the energy is derived from large scale combustion units fed by solid fuels, of which the dominating fuel type is coal [2]. With the recognition of how combustion of fossil fuels affects the environment there has been an increased concern of the CO_2 emissions from the use of fossil fuels [3, 4]. Consequently, efforts to transform the conventional energy conversion processes have increased over the last decades and are expected to continue so. Two examples are the replacement of fossil fuels with biomass and carbon capture and storage technologies. Such measures do, however, imply drastic changes of conventional technologies and call for improved tools, such as modelling to assist the development.

The main techniques used for combustion of solid fuels are grate firing, FB combustion and pulverized coal combustion. Pulverized coal combustion is characterized by large, high efficient boilers that are applied in the high power range [5, 6]. Grate fired boilers are used in the low to medium thermal capacity range and are fed by bulky, often low quality fuels. Compared to pulverized coal combustion, no pretreatment of the fuel is required, however, the efficiency of the boiler type is lower. FB boilers are typically applied in the mid-range of thermal capacities, and can efficiently burn a variety of solid fuels with regard to both fuel composition and size. The main advantages of the combustion technique is the fuel flexibility and the economically efficient solution for flue gas cleaning. The FB combustion technique enables a uniform temperature profile in the furnace and thereby low levels of thermal NO_x. Intrinsic capture of SO_x is also possible by adding limestone to the bed material.

The installed capacity of FB boilers has increased steadily over the last years. In 2009, a $460\,MW_e$[1] circulating fluidized bed (CFB) boiler was taken in operation at the Łagisza Power Station in Poland [7]. At present, work is conducted in order to reach CFB boiler capacities of $800\,MW_e$ [8]. The continued development and scale up of FB boilers require research and development, where an important tool that could assist the development is modelling of the combustion processes. FB combustion is however complex as it involves two phase flow, chemical reactions and heat transfer, all coupled to each other [9]. Detailed modelling of the processes requires a large amount of information as it involves phenomena on many different

---

[1]$460\,MW_e$ corresponds to 460 Megawatts of electricity

scales, which makes the modelling very time consuming. At present, comprehensive modelling of FB combustion involves simplifications, especially with regard to the fluid dynamics.

1.1 Fluidized bed boilers

The principle of a FB boiler is to fluidize a bed of solid particles by the use of a fluid flowing from below [10, 11]. The fluid used is combustion air or a mixture of air and recycled flue gases. The fuel is fed into the particle bed and the main conversion stages of the fuel; drying, devolatilisation and char combustion, take place inside the bed with final burnout of gases above the bed.

The bed material typically consists of inert solids, such as sand, which disperse the heat produced from the combustion reactions. As the gas fed from the bottom of the furnace flows upward, the particles in the bed are affected by drag forces depending on the velocity of the gas [12, 13]. For a certain gas velocity, the frictional forces acting on the particles equal the gravitational forces, and the result is a bed at minimum fluidization, where the solid material behaves as a fluid. Based on the degree of fluidization of the bed material, i.e. the velocity of the gas, a distinction can be made between two different types of fluidized bed combustion: BFB combustion and CFB combustion. In the former, the velocity of the gas is lower than in the latter.

The gas velocity in a BFB is increased from the minimum fluidization velocity enough to cause the emergence of a well defined horizontal surface of the bed with bubbles and gas passages forming in the bed [13]. This was the first type of boiler used for FB combustion. It is mainly applied for small to medium scale combined heat and power production, corresponding to thermal loads of up to 50 MW [14]. An illustration of a BFB boiler can be seen in Figure 1.1.

The lower part of the furnace in a BFB boiler contains the dense, bubbling bed, while the zone above the bed, which is referred to as the free board or the riser, is basically free from bed material [14]. The dense bed can be compared to a liquid containing particle-free bubbles which rise through the bed before they burst on the bed surface [13]. The liquid-like and chaotic behaviour of the bed enables high levels of mixing which increases mass and heat transfer [15]. The movement of particles and gas allows for a good distribution of fuel and oxygen in the bed which improves the combustion process and helps to keep the furnace temperature even and relatively low. The gas velocity is usually within the range of $0.5\text{--}2\,\text{m}{\cdot}\text{s}^{-1}$ and the bed height is $0.4\text{--}1.5\,\text{m}$ [10, 16].
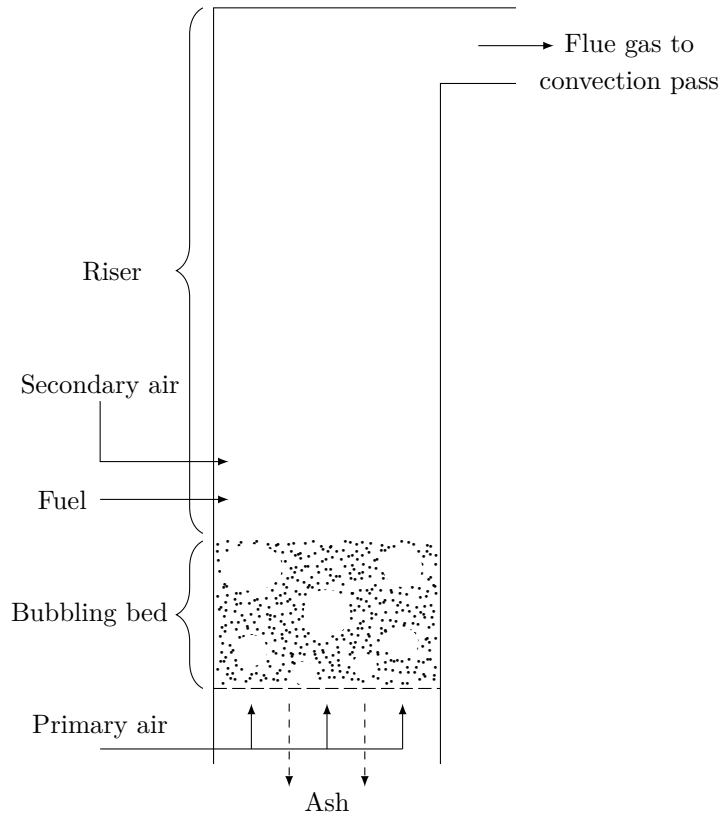
Figure 1.1: *Illustration of a BFB boiler.*

In a CFB the gas velocity is higher, typically 2–5 m·s^{-1}, resulting in that a share of the bed material follows the gas upwards in the riser [16]. Some of the rising particles will reach the upper part of the furnace, where they are transported to one or more cyclones in which gas and particles are separated [10, 15]. The particles are then transported back to the furnace again, resulting in a circulation of bed material. An illustration of a CFB can be seen in Figure 1.2. Compared to a BFB, the bed in a CFB lacks the well defined bubbles in the bed as well as the horizontal surface at the top of the bed. The bed in a CFB is characterized by turbulent movements of gas and particles [13]. Furthermore, the combustion in a CFB boiler is more evenly distributed with regard to the furnace height compared to a BFB boiler, where the majority of the combustion takes place in the bed [14].

Common for the two FB combustion types is to apply staged combustion. Primary air is fed through a distributor in the bottom of the furnace, contributing to the fluidization of the dense bed and supplying oxygen to the combustion process. Above the fuel feeding port, secondary air is injected. The purpose of the staged combustion is to prohibit the formation of NO$_x$ and to ensure complete combustion of volatiles in the riser. In order to enhance complete burnout of the fuel, the combustion process is typically operated using an excess factor of air at 1.2–1.3 [10]. The features of heat extraction in the furnace of FB boilers are governed by keeping the furnace temperature within 800–900 °C [5, 11]. In addition to cooled furnace walls, internal heat exchangers may be implemented in the furnace. Downstream the furnace a convection pass is present where the flue gas is further cooled.
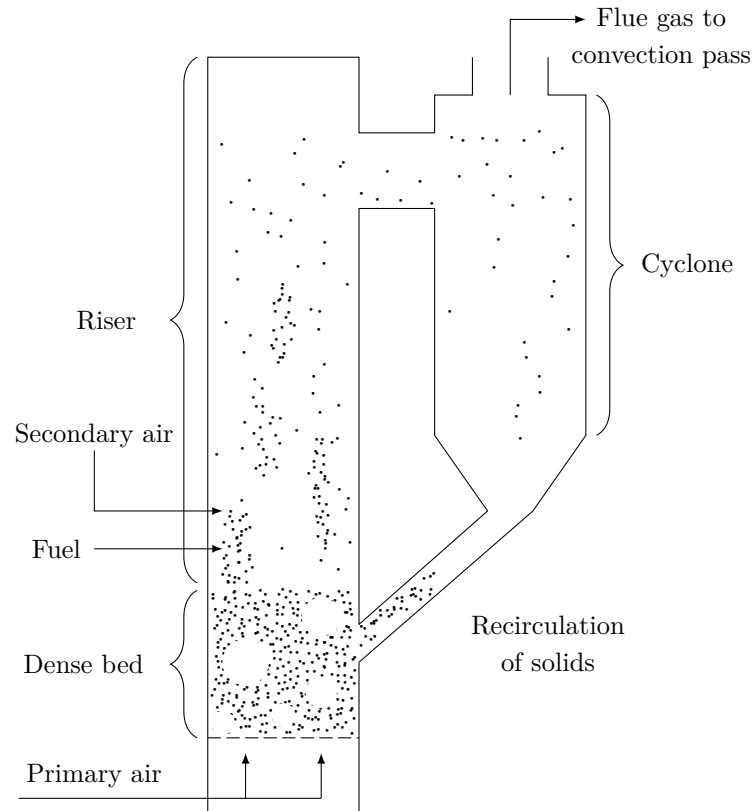
Figure 1.2: *Illustration of a CFB boiler*

1.2 Aim

The aim of this work is to investigate the possibilities of using Comsol Multiphysics for modelling of stationary FB boilers. The modelling work includes the mass and heat transfer in a stationary BFB boiler.

Problems involving the transport of momentum, mass and energy are often solved using commercial computational fluid dynamics (CFD) software, because this enables a flexible and fast implementation. Resolving the details of the two phase flow in a BFB boiler is very computationally demanding, and therefore semi-empirical modelling is commonly used for the fluid dynamics. Many commercial CFD software are, however, not adapted to this kind of modelling, and are therefore not an option unless there are possibilities to implement user defined models.

Another option for semi-empirical modelling of FB combustion is to implement models and solvers with self-developed code. Compared to commercial CFD software, this requires more time and knowledge although it provides the highest degree of flexibility.

Comsol is a commercial software, which offers a high flexibility when it comes to implement and solve transport equations. It could could therefore be a good option for modelling of FB combustion without the need of substantial programming.

2

Theory

This chapter provides an overview of the processes that occur in a BFB boiler, and how these can be modelled. Mixing of gas and solids is described in Section 2.1.1 and a description of the fuel conversion in a BFB is given in Section 2.1.2. Section 2.2 aims to provide an overview of approaches often used for FB modelling. Together with this, the underlying theory used for the work is presented.

2.1 Bubbling fluidized bed combustion

The regions in a BFB boiler involve different mixing and combustion stages. In principle, the dense bottom bed is characterized by two phase flow and accounts for the conversion of the solid phase of the fuel [11]. The dilute riser mainly contains gas where homogeneous reactions take place.

2.1.1 Mixing and motion of gas and solids

The dense bed contains areas with varying amounts of solids and gas. Based on this, it can be considered to consist of two phases: an emulsion and a bubble phase [13]. In regions where cavities and pockets of gas are generated, the solid concentration is low. These areas are considered to belong to the bubble phase, while regions containing both gas and solids belong to the emulsion phase.

The bubble phase consists of gas bubbles of different sizes that are formed and rise upwards, while interacting with each other and with the gas in the emulsion phase [13]. As mentioned in Chapter 1, the chaotic behaviour in the bed enables high levels of mixing with regard to both gas-solid and solid-solid interactions. Eventually the bubbles burst on the bed surface. Above the bed and further up in the riser, the rate of mixing decreases and the flow is often characterized as a plug flow of gas [14].

2.1.2 Fuel conversion

As the fuel particles are fed to the furnace, they are exposed to a temperature of typically 800–900 °C. While the particles are heated they are first dried, then devolatised and finally the exothermic char combustion takes place [17]. During the stages of drying and devolatilisation, moisture and volatile compounds, such as H_2, CO and CO_2, are released. When all moisture and volatiles have left the particle only

char remains. As the particle temperature is sufficiently high, there will be an onset of heterogeneous reactions between the char and the surrounding oxygen. For such reactions to occur, oxygen from the bulk must diffuse through the boundary layer of gas around the particle. The oxygen molecules that reach the particle surface may, depending the porosity and temperature of the particle, be able to diffuse further into the particle before they react with the char.

The high level of solids mixing in the bed contributes to the particles being effectively dispersed while being converted [11]. The rates of drying and devolatilisation are however significantly higher than the char combustion and a share of the volatiles is often released close to the fuel inlet. The fuel is present in the emulsion phase of the bed, where gas is generated due to drying and devolatilisation. Also char conversion and gas phase reactions take place in the emulsion phase, whereas in the bubble phase, only gas phase reactions occur.

2.2 Modelling of fluidized bed combustion

Modelling of FB combustion does in general include the following phenomena: fluid dynamics, mass transfer, chemical reactions and heat transfer. Due to the complex processes occurring in a FB, simplifications are often applied to model these phenomena. This section contains a short summary on FB modelling in general, followed by the theory of the specific models used in this work.

There are different approaches for FB modelling with regard to the amount of information taken into account. Gómez-Barea and Leckner [16] have defined three main approaches

- Computaional fluid dynamics models (CFDM)

- Fluidization models (FM)

- Black box models (BBM)

In CFDM the momentum equations are solved to obtain the velocity fields of solids and gas. They thereby give detailed information about the flow field compared to the other two other approaches where no equations for momentum are solved. Consequently this type of models also requires much more computational time. On the contrary to CFDM, BBM are macroscopic and based on global mass and heat balances. They thereby only give an overall description of the FB boiler, with no information of the processes occurring inside it. The most common approach for comprehensive modelling of FB boilers is to use FM, which is the approach chosen in this work. These models can be considered as hybrids between CFDM and BBM. No momentum equations are solved, and the two phase flow is represented by dividing the gas into an emulsion and a bubble phase. The fluid dynamics of gas and solids are described through transport equations, but by using more simplified approaches, such as semi-empirical correlations and potential flows.

2.2.1 Mass and heat transfer

Modelling of mass and heat transfer is conducted by formulating transport equations for the physical quantities of interest [18]. These equations are derived from a balance of the quantity over an infinitely small volume, accounting for net transport through the boundaries of the volume, generation or consumption in the domain and accumulation within the volume.

The transport of mass and energy is governed by convection and/or diffusion. The convective contribution arises when there is a flow characterized by a macroscopic velocity, while the diffusive transport involves the random movement on a molecular level. For a three-dimensional domain, the transport equation of a variable Φ is given by

$$\frac{\partial \Phi}{\partial t} + u\frac{\partial \Phi}{\partial x} + v\frac{\partial \Phi}{\partial y} + w\frac{\partial \Phi}{\partial z} = D\left(\frac{\partial^2 \Phi}{\partial x^2} + \frac{\partial^2 \Phi}{\partial y^2} + \frac{\partial^2 \Phi}{\partial z^2}\right) + S(\Phi), \qquad (2.1)$$

where Φ is the temperature or the molar/mass concentration of a specie. The first term on the left hand side of the equation describes accumulation of Φ, and the three following terms describe convective transport of the variable. On the right hand side, the first term describes diffusion of Φ, followed by the source term S which includes consumption, generation and/or exchange of the variable due to phase transitions. In order to simplify the modelling it is common to neglect the transient term with the time derivative and only consider the steady state problem. When Φ is taken as the total mass of the system the continuity equation is obtained,

$$\frac{\partial \rho u}{\partial x} + \frac{\partial \rho v}{\partial y} + \frac{\partial \rho w}{\partial z} = 0, \qquad (2.2)$$

where ρ is the density.

2.2.2 Fluid dynamics and mixing

To solve the mass and heat transfer equations the velocity field is needed. The rigorous way to obtain this is to solve the momentum equations, but the complex nature of the two phase flow in fluidized bed combustion makes this highly demanding. Instead more approximate models are commonly applied [9, 14]. In this section, the simplifications and sub models used in this work are presented, they all belong to the FM group.

2.2.2.1 Potential flow

A potential flow approach can be used as a simplified way to describe the velocity field of a fluid [15]. A diffusion equation is first solved for the flow potential ϕ according to

$$\nabla \cdot (-D\nabla\phi) = \sum_n S_n, \qquad (2.3)$$

where D is the diffusion coefficient whose value can be chosen arbitrarily. The right hand side of equation (2.3) takes density variations and phase transitions into account if needed. The boundary conditions are the fluxes at the inlets and the outlets. Once the variable ϕ has been determined, the velocity is obtained according to

$$\vec{u} \propto \nabla \phi. \tag{2.4}$$

2.2.2.2 Bubble and emulsion phase model

The two phase model proposed by Toomey and Johnstone [19] is based on the concept of having a gas in the dense bed that is distributed between a bubble and an emulsion phase. The model assumes that the emulsion phase, which also includes the solids, is at minimum fluidization and that the bubble phase consists of the rest of the gas flow [13].

The interaction between the gas in the bubble and the emulsion phase is accounted for by mass transfer between the two phases. The mass transfer coefficient, K_{be}, is a function of, for example, the bed diameter, the bubble sizes and the velocity of gas in the emulsion and bubble phase. The value of K_{be} is typically found within the range 0.1–$10\,\mathrm{s}^{-1}$ [13, 20].

The distribution of the fluidizing gas between the bubble and emulsion phase at the bottom of the furnace can be expressed by the minimum fluidization velocity, u_{mf}, and the total velocity of the primary air, u_0, according to

$$
\begin{aligned}
x_e &= \frac{u_{mf}}{u_0} \\
x_b &= \frac{u_0 - u_{mf}}{u_0}.
\end{aligned}
\tag{2.5}
$$

The minimum fluidization velocity in a bed occurs when the drag force exerted by the flowing gas equals the gravitational force of the particles, i.e. when the bed is at minimum fluidization. A force balance can then be formulated by means of the pressure drop over the bed and the bed porosity, ϵ_{mf}, according to

$$\Delta P_b = H_{mf}(1 - \epsilon_{mf})(\rho_s - \rho_g)g, \tag{2.6}$$

where H_{mf} is the bed height at minimum fluidization, ρ_s is the density of the solids, ρ_g is the density of gas and g is the gravitational constant [12]. In order to correlate the velocity and the pressure drop, the Ergun equation [21] is combined with equation (2.6). The solution of the obtained equation with regard to u_{mf} can then be obtained using the correlation of Wen and Yu [13, 22]

$$Re_{p,mf} = \left((28.7)^2 + 0.0408Ar\right)^{1/2} - 33.7, \tag{2.7}$$

where $Re_{p,mf}$ is the Reynolds number of the solids and Ar is the Archimedes number.

2.2.2.3 Dispersion model

A dispersion model describes the movement of a fluid or a particle in a FB by diffusion only, with an experimentally determined dispersion coefficient [23]. It is often applied for describing the movement of fuel and solids in the bed, which is caused by the interaction of gas bubbles and bed material. On a larger scale, the movement acts as random mixing and can be represented as a diffusion process. The dispersion coefficient can be seen as a measure of how well the fuel is transported in the bed and it takes both convective and diffusive transport of the fuel into account.

The transport is more limited in the lateral than in the vertical direction, and the value of the dispersion coefficient is therefore higher in the vertical direction than in the lateral [24]. Values for the lateral direction have been investigated by Sette [23] and lie typically within the range of 10^{-3}–$10^{-1}\,\mathrm{m^2 \cdot s^{-1}}$ depending on the operational conditions.

3

Model structure

The model of this work can be compared to what Gómez-Barea and Leckner [16] have defined as a fluidization model. The model describes the mass and heat transfer in a BFB boiler operating at steady state. The gas in the bottom bed is distributed into an emulsion and a bubble phase. For the fuel conversion, drying, devolatilisation, char combustion and gas phase reactions are considered. The transport equations are coupled through the source terms describing chemical reactions and phase transitions.

3.1 Mass transfer

The mass transfer includes transport of the gaseous species, in both the bubble and the emulsion phase, as well as transport of the fuel components, which in this model are treated as separate flows.

3.1.1 Gaseous species

The mass transfer of gas in the bed is described by a component balance for each gas specie i in the bubble (b) and the emulsion (e) phase respectively, according to

$$\nabla \cdot (-D_{g_b} \nabla C_{i_b} + \vec{u}_{g_b} C_{i_b}) = S_{i,r_b} + S_{i,be} \tag{3.1}$$

and

$$\nabla \cdot (-D_{g_e} \nabla C_{i_e} + \vec{u}_{g_e} C_{i_e}) = S_{i,r_e} - S_{i,be} + S_{v_i} + S_m, \tag{3.2}$$

where C_i is the molar concentration of the specie, D_g is the dispersion coefficient and $\vec{u}$ is the velocity field of the gas. Since the flow of gas is directed upwards, convection dominates the mass transport in the vertical direction. In the lateral direction, the dispersion coefficient governs the mixing which is due to both convection and diffusion. The value of the dispersion coefficient is taken as $0.001\,\mathrm{m}^2{\cdot}\mathrm{s}^{-1}$ and $0.1\,\mathrm{m}^2{\cdot}\mathrm{s}^{-1}$ in the lateral and the vertical direction, respectively [5]. The source term $S_{i,r}$ is the change in the species concentration due to chemical reactions and is given by

$$S_{i,r} = -\sum_j \nu_{i,j} r_j \tag{3.3}$$

for the emulsion phase and the bubble phase respectively, where r_j the reaction rate of reaction j and $\nu_{i,j}$ is the corresponding stoichiometric coefficient for gas specie i.

When O_2 or CO_2 are considered in the emulsion phase, the source term S_{i,r_e} also includes terms to account for char conversion.

The second source term on the right hand side of equation (3.1) and (3.2) accounts for transfer of the species between the bubble and the emulsion phase,

$$S_{i,be} = K_{be}(C_{i_e} - C_{i_b}),$$ (3.4)

where the value of K_{be} is taken as $0.5\,\mathrm{s}^{-1}$. [13, 20]. The last two source terms on the right hand side of equation (3.2), S_m and S_{v_i}, account for drying and devolatilisation. A further description of the source terms is given in Section 3.2.

The inlet boundary conditions for equation (3.1) and (3.2) are the molar fluxes of the species. The total molar flux of combustion air required is scaled by the fractions x_b and x_e to yield the molar flux of O_2 and N_2 entering the bubble and the emulsion phase, respectively. The outlet boundary condition is an outflow: $D_g \nabla C = 0$. In the riser only one gas phase is considered. The transport equation solved for each specie in this part of the furnace is given by

$$\nabla \cdot (-D_i \nabla C_i + \vec{u}_g C_i) = S_{i,r},$$ (3.5)

where $S_{i,r}$ includes the gas phase reactions and $\vec{u}_g$ is the velocity of gas in the riser.

3.1.2 Solid species

Component balances of the fuel species are obtained using the dispersion model presented in Section 2.2.2.3. For the moisture (m) and the volatile species (v_i), the mass balances are given by

$$\nabla \cdot (-D_f \nabla C_m) = S_m$$ (3.6)

and

$$\nabla \cdot (-D_f \nabla C_{v_i}) = S_{v_i},$$ (3.7)

where D_f is the dispersion coefficient of the fuel which is taken as $0.05\,\mathrm{m}^2{\cdot}\mathrm{s}^{-1}$ in the lateral direction, and $0.5\,\mathrm{m}^2{\cdot}\mathrm{s}^{-1}$ in the vertical direction [23, 25]. Volatiles and moisture leaving the fuel are accounted for in the source terms S_{v_i} and S_m.

The equation describing the mass transfer of char is

$$\nabla \cdot (-D_f \nabla C_{c_k}) = S_{c_k,r},$$ (3.8)

where the source term corresponds to the char conversion, which is modelled using five char classes [20]. Equation (3.8) is thus formulated for each char class c_k, where C_{c_k} is the molar concentration of char class k. The inlet boundary conditions are molar fluxes of the species. The other surfaces in the bed are defined by a Neumann boundary condition. The char conversion and the source terms are further described in the following section.

3.2 Chemical reactions and phase transitions

This section contains a description of the fuel conversion, which is accounted for by source terms in the equations formulated for the gas and the fuel.

3.2.1 Drying and devolatilisation

The source terms in equations (3.6) and (3.7) account for the drying and devolatilisation and are given by

$$S_m = -\nu_m r_m \tag{3.9}$$

and

$$S_{v_i} - \nu_{v_i} r_{v_i}. \tag{3.10}$$

The rate expressions for the moisture and volatile release are

$$r_m = -k_m \frac{T}{T_{ref}} \frac{d_{p,ref}}{d_p} C_m \tag{3.11}$$

and

$$r_{v_i} = -k_{v_i} \frac{T}{T_{ref}} \frac{d_{p,ref}}{d_p} C_{v_i}, \tag{3.12}$$

where k is the rate constant, T_{ref} is the reference temperature of $1123\,\mathrm{K}$, $d_{p,ref}$ is the reference particle diameter of $1\,\mathrm{cm}$ and C is the molar concentration of moisture or volatile species [20]. The actual particle diameter d_p corresponds to an arithmetic mean value of the initial size of the fuel particles and the size after drying and devolatilisation. The values chosen for k_m and k_{v_i} are $0.05\,\mathrm{s}^{-1}$ and $0.02\,\mathrm{s}^{-1}$, respectively [20]. The volatiles are assumed to consist of CO, H_2 and CO_2 for which the distribution is given in Table 3.1.

Table 3.1: *Distribution of the volatiles assumed for the fuel.*

Specie	Mass fraction
CO	0.3
H_2	0.1
CO_2	0.6

3.2.2 Gas phase reactions

The gas phase reactions considered are

$$CO + 1/2 O_2 \rightarrow CO_2$$
$$H_2 + 1/2 O_2 \rightarrow H_2O \tag{3.13}$$

with the reaction rates described by [26, 27]

$$r_{CO} = 1.3 \cdot 10^8 C_{O_2}^{0.5} C_{H_2O}^{0.5} C_{CO} \exp\left(\frac{-15100}{T}\right)$$
$$r_{H_2} = 1.3 \cdot 10^{11} C_{H_2} C_{O_2} \exp\left(\frac{-5050}{T}\right).$$

(3.14)

3.2.3 Char conversion

Char combustion is assumed to proceed according to

$$C + O_2 \rightarrow CO_2.$$

(3.15)

The conversion is described by using five classes of char with decreasing size and thereby different reaction rates [20]. Each class is defined by the actual particle size. This means that the first class is defined by the particle size before char combustion has started. The source term, $S_{c_k,r}$, of equation (3.8) describes the conversion of class k caused by combustion, and is given by

$$S_{c_k,r} = \frac{V_{c_k}\rho_c}{M_c}(\dot{p}_{c_{k-1}} - \dot{p}_{c_k}),$$

(3.16)

where V_{c_k} is the actual particle volume of char class k, M_c is the molar mass of carbon, ρ_c is the char density and $\dot{p}$ is the number of char particles being converted per class and second. As the char of class k is combusted, it gives rise to a flow of particles entering the next class, $k + 1$. Correspondingly, the rate of particles entering class k is the same as those leaving class $k - 1$. The rate of the particles entering and leaving class k, respectively, are given by

$$\dot{p}_{c_{k+1}} = \frac{M_c r_{c_{k+1}}}{V_{l_{c_{k+1}}}\rho_c}$$
$$\dot{p}_{c_k} = \frac{M_c r_k}{V_{l_{c_k}}\rho_c},$$

(3.17)

where V_l is the volume of the char layer of the class. The reaction considered for the conversion is given by equation (3.15), where the amount of CO_2 generated for each class transition is given by the difference in mass between two subsequent classes

$$S_{CO_2} = \frac{\dot{p}_{c_{k+1}}\rho_c}{M_c}\left(V_{c_{k+1}} - V_{c_k}\right).$$

(3.18)

The total molar generation of CO_2 is thus obtained by a summation over all class transitions, and is implemented in the source term given by equation (3.3).

A simplified mechanism is used to describe the char conversion based on the assumption that the oxygen is consumed on the surface of the char particle. Thus, the reaction rate of the heterogeneous reaction is regarded as infinitely fast compared to the transport of oxygen within the particle. This is reasonable for the high temperatures of interest here. Since no oxygen will diffuse through the particle, the density will remain constant. In addition, any ash layer formed around the particle is neglected due to the interaction between particles and bed material. This corresponds to a case of char conversion referred to as the shrinking sphere model, for which the reaction rate is given by [17]

$$r_{c_k} = -n_{p_{c_k}} \Omega_{c_k} A_{p_{c_k}} k_{r_{eff_{c_k}}} C_{\text{O2},\infty}, \tag{3.19}$$

where n_p is the number of particles per furnace volume of class k, given by

$$n_{p_{c_k}} = \frac{C_{c_k} M_c}{\rho_c V_{c_k}}. \tag{3.20}$$

Ω is the stoichiometric number of moles of carbon divided with those of oxygen required for the reaction, A_p is the particle surface area and $C_{O_2,\infty}$ is the bulk concentration of oxygen. The effective rate constant, $k_{r_{eff}}$, takes the transport of oxygen through the external gas film into account, together with the kinetics of the reaction

$$k_{r_{eff}} = \frac{k_r h_m}{k_r + h_m}, \tag{3.21}$$

where k_r is the reaction rate constant given by the Arrhenius expression,

$$k_r = A \exp\left(\frac{-E_A}{RT}\right), \tag{3.22}$$

with the pre-exponential factor obtained from

$$A = 10^{(0.2 \cdot 10^{-4} E_A + 2)}, \tag{3.23}$$

where E_A is the activation energy. The second variable on the right hand side of equation (3.21), h_m, is the mass coefficient which contains information about the transport of oxygen to the particle surface. It is obtained using the Ranz-Marshall correlation [28],

$$Sh = \left(2 + 0.6 Re^{0.5} Sc^{1/3}\right). \tag{3.24}$$

3.3 Gas velocity

The velocity field corresponding to gas in the bubble and emulsion phase, respectively, is obtained using the potential flow approach, which is described by equations (2.3) and (2.4) in Section 2.2.2. The value of the dispersion coefficient in the vertical direction is chosen arbitrarily, while that in the lateral direction is $0.001\,\text{m}^2\cdot\text{s}^{-1}$ [5]. The source terms of equation (2.3) are given by

$$\sum_n S_{n_b} = \sum_i S_{i,r_b} + \sum_i S_{i,be} \tag{3.25}$$

for the bubble phase, and

$$\sum_n S_{n_e} = -\sum_i S_{i,r_e} - \sum_i S_{i,be} + \sum_i S_{v_i} + S_m \tag{3.26}$$

for the emulsion phase. The flow potential is defined as the total molar concentration of gas in the bubble and the emulsion phase respectively. By using the ideal gas law, the velocity of each phase is given by

15

$$\vec{u} = \frac{RT}{P} D_g \nabla C. \tag{3.27}$$

In the riser, equation (2.3) is solved for the total concentration of gas with the source term given by

$$S = \sum_i S_{i,r}. \tag{3.28}$$

3.4   Heat transfer

All solids species are assumed to have the same temperature as the gas, and therefore only one heat balance is formulated, according to [20]

$$\rho_g C_{p_g} (\vec{u_{g_b}} + \vec{u_{g_e}}) \nabla T = \nabla \cdot (\lambda_{bm} \nabla(T)) + \dot{q}_r, \tag{3.29}$$

where ρ_g is the density of the gas and C_{p_g} is the heat capacity of the gas. The heat conductivity accounts for conduction and dispersive mixing of bed material according to

$$\lambda_{bm} = D_{bm} C_{p_{bm}} \rho_{bm}, \tag{3.30}$$

where D_{bm} is the dispersion coefficient of the bed material which is taken as $0.05\,\mathrm{m^2 \cdot s^{-1}}$ and $0.5\,\mathrm{m^2/s}$ in the lateral and the vertical direction, respectively [23]. Furthermore, $C_{p_{bm}}$ is the heat capacity, and ρ_{bm} is the density of the bed material, given by

$$\rho_{bm} = \epsilon_{bed} \rho_s, \tag{3.31}$$

where ρ_s is the density of the solid particles and ϵ_{bed} is the bed voidage, which is estimated to be 0.43 by using the Ergun equation [21].

The source term, $\dot{q}_r$, on the right hand side of equation (3.29) includes the heat required for phase transitions and the heat released from the chemical reactions, and is given by

$$\dot{q}_r = -\sum_j \nu_{j_e} r_{j_e} \Delta H_{r_j} - \sum_j \nu_{j_b} r_{j_b} \Delta H_{r_j} - \sum_i \nu_{v_i} r_{v_i} \Delta H_{v_i} - \nu_m r_m \Delta H_m, \tag{3.32}$$

where ΔH is the heat of reaction and ν is the number of moles of product formed per mole reaction. The corresponding equation solved for the riser is

$$\rho_g C_{p_g} \vec{u_g} \nabla T = \nabla \cdot (\lambda_g \nabla(T)) + \dot{q}_{r_{riser}}, \tag{3.33}$$

where $\dot{q}_{r_{riser}}$ is the source term which accounts for the heat released due to the gas phase reactions,

$$\dot{q}_{r_{riser}} = \sum_j \nu_j r_j \Delta H_{r_j}. \tag{3.34}$$

The inlet boundary conditions for the energy equations are temperatures, and the outlets are defined as outflows; $\nabla T = 0$. The boundary condition for the walls is a convective flux

$$\dot{Q}_w = h_h(T - T_w), \tag{3.35}$$

where h_h is the heat transfer coefficient and T_w is the wall temperature.

4

Simulations

Section 4.1 aims at providing the basics of how the implementation and simulation of a model is conducted in Comsol, and in Section 4.1.1, the numerical method used in Comsol is described. In Section 4.2, the setup used for the modelling in Comsol is described. Finally, Section 4.3 contains a description of the reference case which was used for the simulations.

4.1 Features of Comsol

The transport equations, together with boundary conditions and physical properties are implemented in Comsol by using so called *physics interfaces*. An interface defines a set and the type of equations to be solved, and their variables [29]. The interfaces used for the mass balance and the heat balance in this work are *Transport of Diluted Species* and *Heat Transfer in Fluids*, respectively. In the former, the number of species considered is defined, which yields the same number of equations to be solved for the species molar concentrations. In the *Heat Transfer in Fluids* interface, the only variable solved for is the temperature.

The variables that the equations of the interfaces are solved for are referred to as *Dependent Variables*. The dependent variables have default names and definitions in Comsol. User defined expressions can be derived from the dependent variables, and be defined in lists as *Variables* in Comsol. Apart from variables, a list of *Parameters* can also be defined. The difference between variables and parameters is that the parameters are constant.

The equations of the interfaces are solved in a *Study*. Depending on whether the problem is stationary or time dependent, a stationary or a time dependent study type is chosen. The interfaces, i.e. which equations, that are included in the study can be chosen arbitrarily. Several studies can also be defined. From each simulated study the solution can be stored and defined as initial values for a following study. Furthermore, an auxiliary parameter sweep for a simulation can be conducted in a study. This means that an interval of a parameter present in an interface is defined, for example a psychical property or a Dirichlet boundary condition value. When running the study, Comsol solves automatically the equations for parameter values within the interval. The auxiliary sweep can thus be used for sensitivity analysis, but also to enhance convergence. This is because the solution from the previous parameter value is saved and used as an initial guess for the simulation of the next

parameter value. More information about setting up a model in Comsol can be found in Appendix A.

4.1.1 The finite element method

Equations in modelling are often impossible or very hard to solve analytically. Numerical methods for solving the equations are then required. The numerical method used in Comsol is the finite element method (FEM), which enables the problem to be described by a linear system of equations. This is done by discretizing the domain by dividing it into several cells. Piece-wise linear functions are then defined in each cell and the differential equation to be solved is re-formulated. A solution is obtained from a linear combination of the defined functions and the final, approximate solution obtained for the problem consists of the joint solutions for all cells. [30]

4.2 Setup in Comsol

The bed and the riser were modelled using separate interfaces. This was conducted in order to model the transition from the two phase flow of gas in the bottom bed, to the single phase flow in the riser. In the bed, five *Transport of Diluted Species* interfaces were used. For the bubble phase, one interface was used for the gas velocity and one for the mass transfer. The same approach was used for the emulsion phase. Thus, four interfaces were defined for the gas in the bed, whereas the fifth interface was defined for the fuel species. In the riser, two *Transport of Diluted Species* interfaces were used: one for the gas velocity and one for the species. Finally, one *Heat Transfer in Fluids* interface was used for the heat balance of the furnace. The total number of interfaces was eight.

The inlet boundary conditions of the riser were defined by the outlet conditions of the bed. This was conducted by adding the molar fluxes of species in the bubble and the emulsion phase at the interface between the bed and the riser. In total, three studies were used for the simulations. The first study was defined for the mass balance of the bed. The solution obtained was then used in the following study, where the mass balance of the bottom bed and the riser were simulated simultaneously. The temperature used for the isothermal simulations was $1123\,\mathrm{K}$. Finally, in the third study, the mass balance of the bottom bed and the riser were coupled to the heat balance. The reason for simulating the mass balance of the bottom bed in the first study was to reduce the simulation time and to enhance convergence. The structure of the solution process can be seen in Figure 4.1.
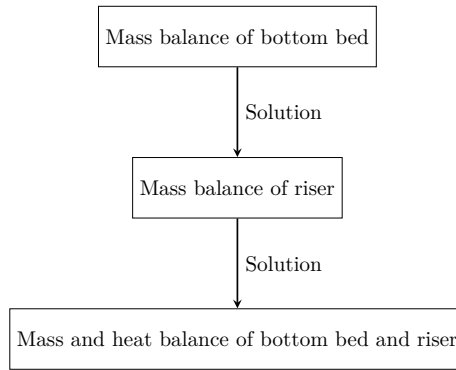
Figure 4.1: *Flowchart of the solution process in Comsol where each step corresponds to a study.*

4.3 Reference case

The geometry used was based on the furnace of a 20 MW BFB boiler, operated by Borås Energi, and can be seen in Figure 4.2. In Table 4.1 the dimensions of the furnace are given. The mesh was constructed as a physics controlled mesh. This means that Comsol conducts the meshing of the domain automatically and adapts it based on the equations to be solved. The mesh was manually refined at the interface between the bottom bed and the riser in order to obtain accurate molar flows to the riser, since the accuracy of these are mesh dependent.

Table 4.1: *Furnace dimensions.*

H_{bed}	0.7 m	Height of bottom bed
H_{riser}	11.3 m	Height of riser
H_{sa}	3.35 m	Height of secondary air inlets
W	4 m	Width of furnace
D	5 m	Depth of furnace

The fuel composition is given in Table 4.2. The heating value was $11.32\,\mathrm{MJ \cdot kg^{-1}}$ and the ash-free fuel was used in the simulations. The initial particle diameter was 2.3 cm, yielding a particle diameter of the first char class of 1 cm. For each class, the diameter was set to decrease by 25% compared to the previous.

Table 4.2: *Fuel composition on an as received mass basis.*

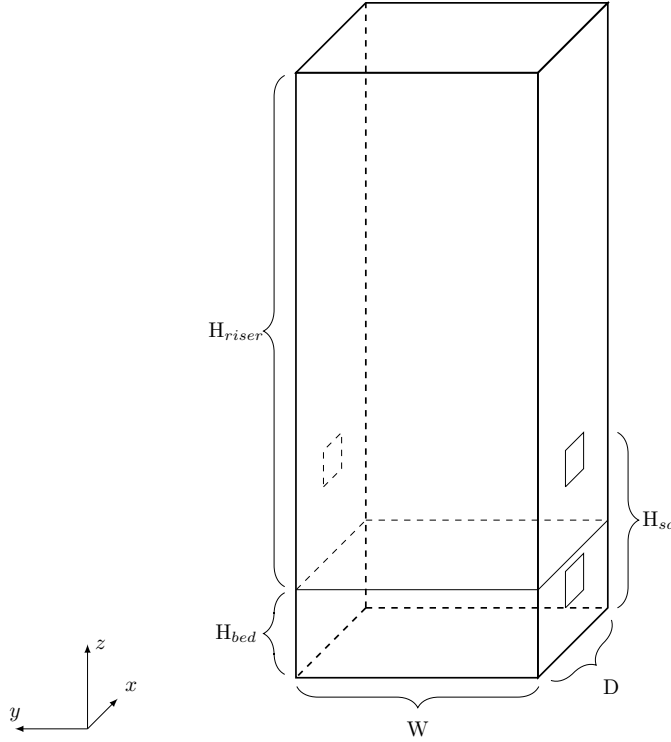| Specie	Mass fraction
Moisture	0.30
Volatiles	0.55
Char	0.10
Ash	0.05

Figure 4.2: *Geometry of the furnace where the lower section is the bottom bed, and the upper section is the riser. The rectangular surface located on the right hand side of bottom bed is the fuel inlet. The two rectangular surfaces in the riser are the secondary air inlets.*

The excess air ratio was 1.3 and the volumetric flow rate of primary and secondary air was $4.6\,\mathrm{Nm^3 \cdot s^{-1}}$ and $2.5\,\mathrm{Nm^3 \cdot s^{-1}}$, respectively. Silica sand, SiO_2, was used as bed material for which the properties are given in Table 4.3 [31].

Table 4.3: *Properties of the bed material (SiO_2).*

Property	Symbol	Expression	Unit
Diameter	d_s	200	μm
Density	ρ_s	2600	$\mathrm{kg \cdot m^{-3}}$
Heat capacity	C_{p_s}	$28.68 + 0.05680T$	$\mathrm{J \cdot mole^{-1} \cdot K{-}1}$

Transport properties used for the gas are given in Table 4.4 [31]. The diffusivity in the riser was taken for O_2 in air, and the thermal conductivity and the heat capacity for air.

Table 4.4: *Transport properties of the gas.*

Property	Symbol	Expression	Unit
Diffusivity	D_g	$18 \cdot 10^{-6}(T/298)$	$\mathrm{m^2 \cdot s^{-1}}$
Thermal conductivity	k_g	$2.44 \cdot 10^{-2}(T/273)$	$\mathrm{W \cdot m^{-1} \cdot K^{-1}}$
Heat capacity	C_{p_g}	$29.4986 + 0.00316T$	$\mathrm{J \cdot mole^{-1} \cdot K{-}1}$

For the heat balance, the inlet temperature of the primary air was 300 K. The wall temperature of equation (3.35) was 600 K and the heat transfer coefficient was $110 \, \text{W·m}^{-2} \cdot \text{K}^{-1}$.

5

Results and discussion

Section 5.1 of this chapter contains a discussion regarding the results obtained from the simulations conducted for the reference case. Due to problems with implementing the heat balance, the simulation results given are those for the mass balance only. The problems obtained during the implementation of the heat balance are further discussed in Chapter 6.

Four different planes are used for the presentation of the figures in this chapter. The planes are defined and named according to Figure 5.1 and 5.2, respectively.
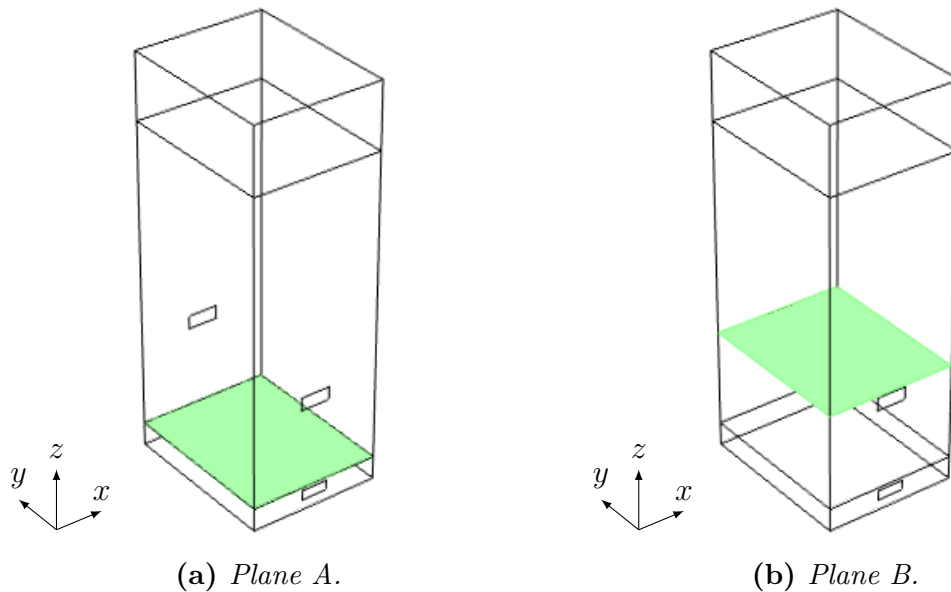

(a) *Plane A.*   **(b)** *Plane B.*

Figure 5.1: *Definition of plane A and plane B used for the visualization of the results throughout this chapter.*

(a) *Plane C.* **(b)** *Plane D.*

Figure 5.2: *Definition of plane C and plane D used for the visualization of the results throughout this chapter.*

5.1 Reference case

Because the heating of the particles is not included in the model, a large share of the reactions and phase transitions occur close to the fuel inlet. This is the case for drying and devolatilisation, of which the rates are highest close to the fuel feeding port and decrease along the depth of the furnace. This can be seen from Figure 5.3 which shows the sum of the rates of drying and devolatilisation in Plane D. The constant temperature implies that the variation of the rates is only due to the decreasing concentration of the volatiles and moisture in the fuel.

Figure 5.3: *The sum of the rates of drying and devolatilisation ($mole \cdot m^{-3} \cdot s^{-1}$) in plane D. The fuel feeding port is located to the right.*

In Figure 5.4 the concentration profiles of particles of the first char class can be seen, together with the flux vectors. The fuel is fed to the bed at the front side of the plane, from which the char concentration decreases as the particles diffuses further into the furnace. Similar to the rate of drying and devolatilisation, the rate of char conversion is largest close to the fuel feeding port.
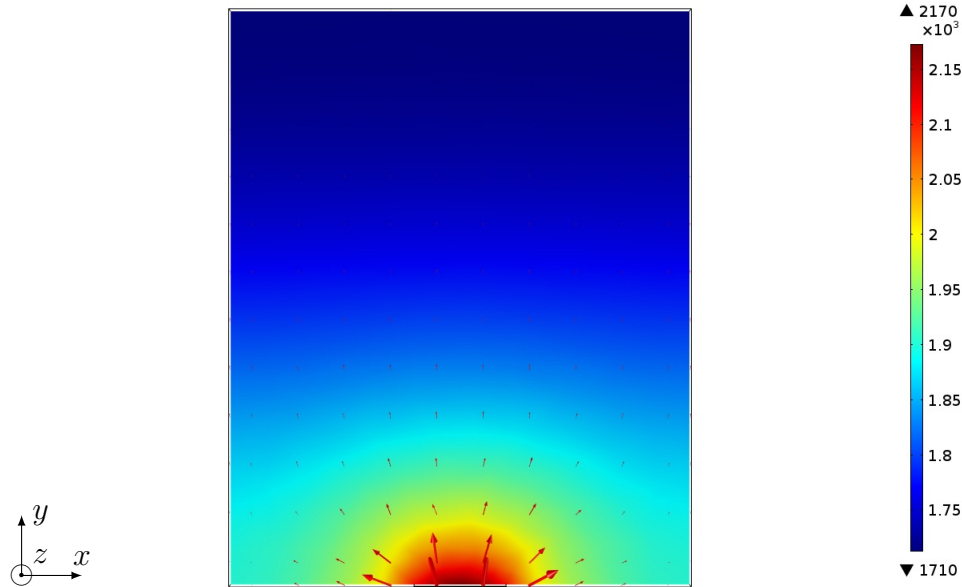

Figure 5.4: *Concentration of the first char class (mole·m^{-3}) together with the molar flux vectors (mole·m^{-2}·s^{-1}) in plane C. The fuel feeding port is located at lower side of the figure.*

Figure 5.5 shows the rate of char conversion for the first class. It can be seen that the largest reaction rates of the char conversion are found close to the fuel feeding port where the concentration of the char is high, and close to the air inlet where the concentration of O_2 has its maximum.

The fractions of air entering the bubble- and the emulsion phase are $x_b = 0.935$ and $x_e = 0.065$ respectively. A net molar flow of O_2 occurs from the bubble to the emulsion phase in the entire bed. This is due to the concentration of O_2 in the bubble phase being is larger than in the emulsion phase, together with the consumption of O_2 in the emulsion phase due to the char conversion. Furthermore, the oxidation of H_2 occurs to a greater extent in the bubble phase than in the emulsion phase. For CO, the oxidation takes place entirely in the bubble phase as explained below. This can be seen from Table 5.1 where the distribution of volatiles, char and O_2 converted in each phase of the bed are given.
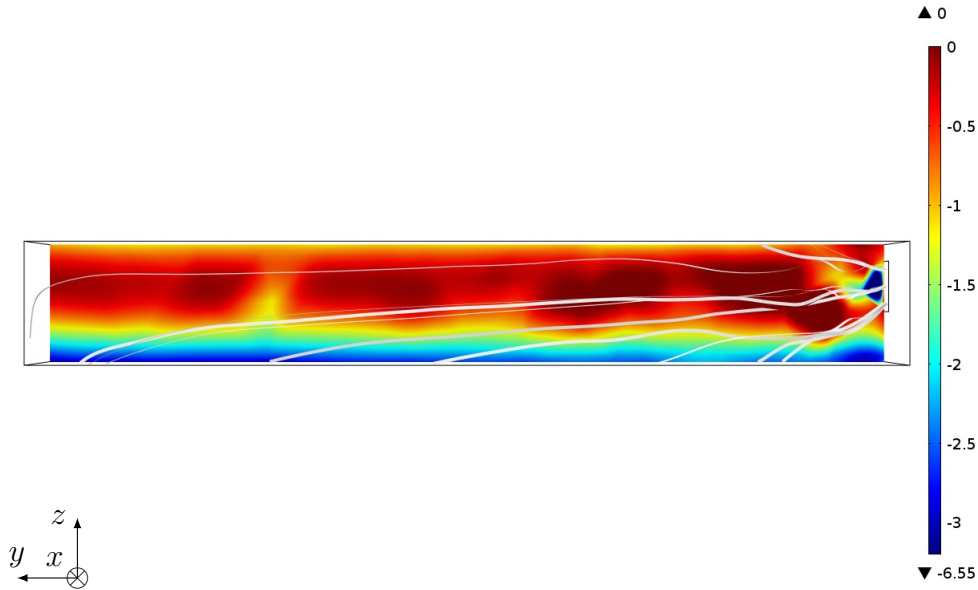
Figure 5.5: *Rate of char consumption (mole·m^{-3}·s^{-1}) together with the streamlines of the particle in plane D. The negative sign indicates that char is consumed.*

Table 5.1: *Distribution of the consumption of char, volatile species and O_2. The second row shows the consumption that takes place in the bottom bed, related to the total consumption in the furnace. In the following two rows, the distribution of the consumption in the bed is given with regard to the two phases.*

Reactant	Char	O_2	CO	H_2
Consumption in bottom bed	100%	72%	53%	59%
Consumption in bubble phase	0%	40%	100%	76%
Consumption in emulsion phase	100%	60%	0%	24%

As devolatilisation takes place in the emulsion phase, there is a net flow of CO and H_2 transported from the emulsion phase to the bubble phase. A share of the H_2 reacts in the emulsion phase with the O_2 available in this phase. This reaction consumes all of the O_2 available in the emulsion phase and, therefore, no reaction occurs for CO. The reason for this is that the reaction rate of H_2 is much higher than that of CO, and therefore dominates. In the bubble phase, however, there is a molar flow of O_2 leaving the bed into the riser and all of the O_2 and H_2 entering this phase is consumed. Thus, it seems as the mass transfer rate between the phases is not high enough to supply O_2 to the emulsion phase for both the CO and the H_2 oxidation to be fully combusted there.

Figure 5.6 shows the concentration profile of O_2 for both phases together. As can be seen, the O_2 consumption close to the fuel inlet is high, which is caused by the oxidation of H_2 and CO. When viewing the O_2 concentration profile from plane D, the concentration profile shows a pattern that is consistent with the char consumption rate shown in Figure 5.5; it has its maximum in the bottom of the bed and
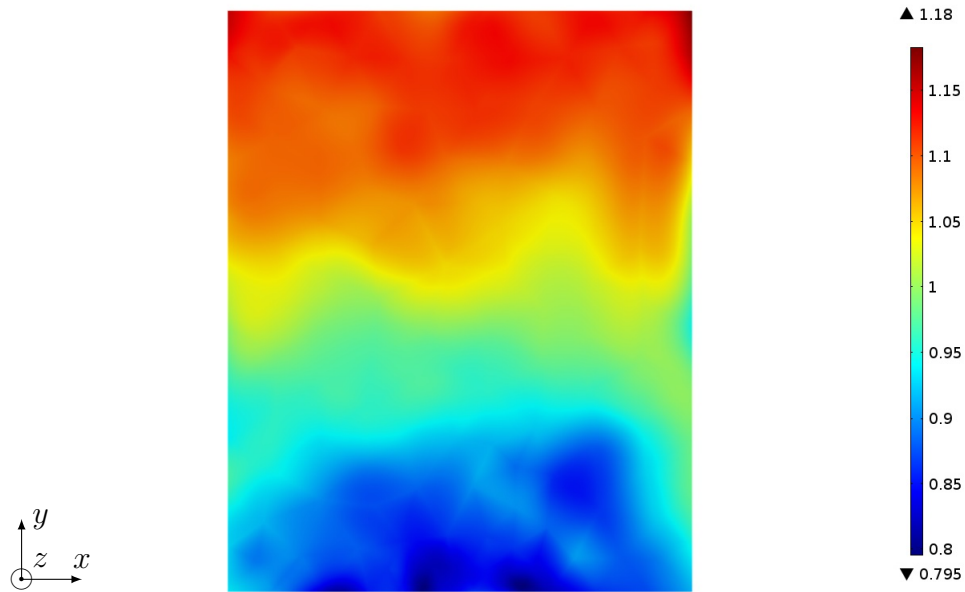
decreases with the bed height.

Figure 5.6: *Concentration profile of O_2 (mole·m^{-3}) for both phases together in Plane A. The fuel feeding port is located at the lower side of the figure.*

The velocity fields obtained for the two phases can be seen in Figures 5.7 and 5.8. The largest changes are in the emulsion phase, especially close to the fuel feeding port.
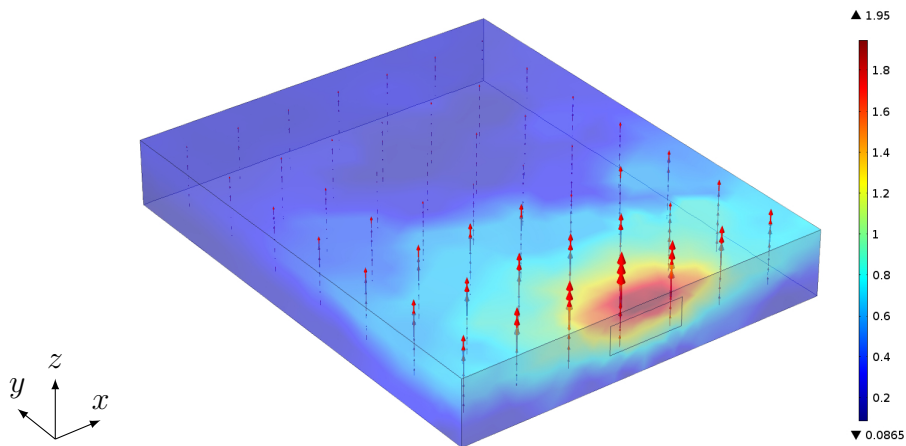

Figure 5.7: *Velocity of the emulsion phase (m·s^{-1}) together with the molar flux vectors (mole·m^{-2}·s^{-1}). The fuel feeding port is the rectangular surface located at the lower right hand side of the figure.*
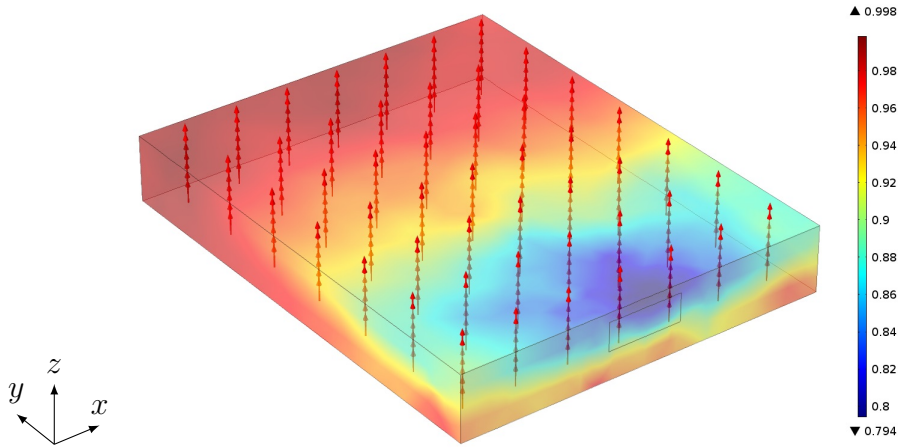
Figure 5.8: *Velocity of the bubble phase (m·s^{-1}) together with the molar flux vectors (mole·m^{-2}·s^{-1}). The fuel feeding port is the rectangular surface located at the lower right hand side of the figure.*

It can be seen from the figures that the two phases exhibit opposite variations in the velocity, i.e, the velocity of the emulsion phase is highest where the velocity of the bubble phase is lowest. Starting with the emulsion phase, the region where the velocity reaches a maximum is where the drying and the devolatilisation occurs. Although a share of the moisture and volatiles are transported to the bubbles, more than half of the produced molar flow is left in the emulsion phase. In the same region, the bubble phase reaches its minimum velocity which implies a contraction of the gas in this phase. Excluding the O_2 consumed during char conversion, more than half of the molar flow of O_2 present in the bubble phase is transferred to the emulsion phase. Also, the oxidation of CO and H_2 implies a net decrease of gas molecules. These reactions have their maximums in the region of the contraction, and in addition occur mainly in the bubble phase.

For the riser, the reaction rates of H_2 and CO had to be reduced by a factor of 10^{-7} and 10^{-1}, respectively, due to convergence problems. Despite this, both species are completely consumed in this domain. Mixing phenomena has, however, not been accounted for and it can therefore be anticipated that the reaction rates are over predicted. The reaction rates are highest at the inlet of the riser and close to the secondary air inlets. Figure 5.9 and 5.10 show the concentration profiles of H_2 in plane A and plane B, respectively. At the bed surface, the concentration is highest in the region above the fuel feeding port and decreases close to the secondary air injection, where the final H_2 is combusted. A similar pattern is observed for CO.

Figure 5.9: *Concentration profile of H_2 (mole·m^{-3}) in plane A. The fuel feeding port is located in the lower part of the figure.*

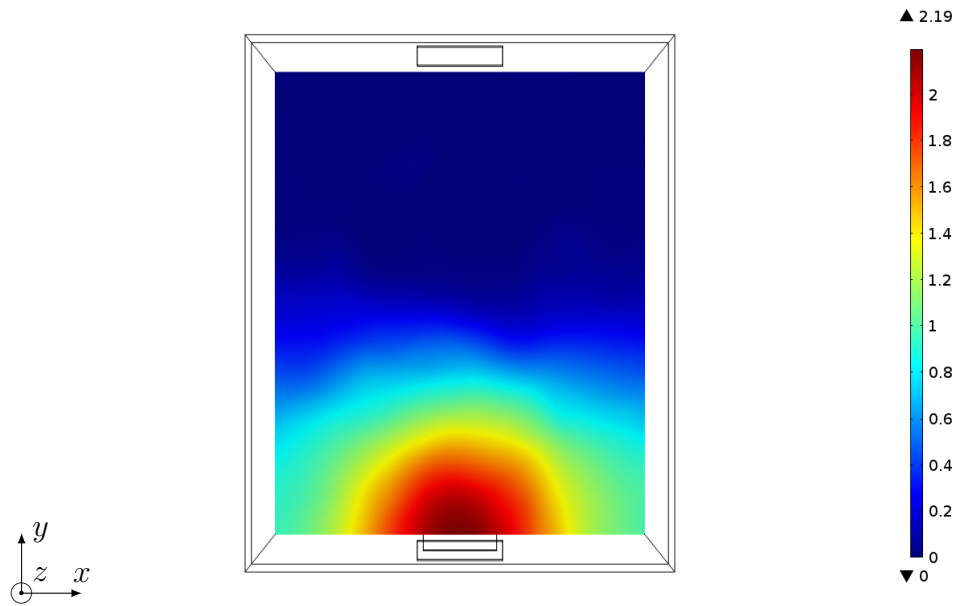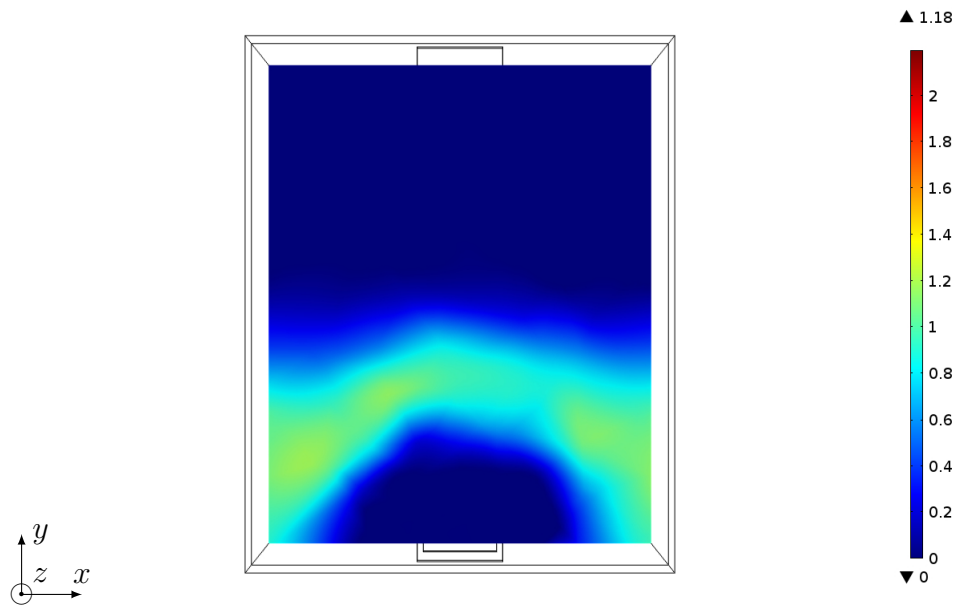**Figure 5.10:** *Concentration profile of H_2 (mole·m^{-3}) in plane B. The fuel feeding port is located in the lower part of the figure.*

6

Experiences of Comsol

This chapter focuses on a discussion concerning the outcome of using Comsol for the simulations. In section 6.1, the problems encountered regarding convergence are presented and discussed, followed by a discussion regarding the implementation of the heat balance in Section 6.2.

Overall, Comsol provides a flexible way of implementing models like the one defined in this work. The main challenge is to gain the knowledge required to find a suitable way to do it. There is a large variety of possibilities in the program, which has been an asset as well as an obstacle for finding suitable ways of implementation. Experience from this work reveals that it is easy to become locked in to only one way of implementing the problem, and due to lack of knowledge not being able to fully realize or understand other possibilities that are available.

The recommended way of obtaining velocity fields in Comsol is to solve the momentum equations and create couplings between these and the mass and heat transfer. For the potential flow method used in this work, it is required that one gains knowledge about which couplings that are taken into account and how this is done by Comsol. A risk may otherwise be that the problem is not properly defined which can give rise to convergence issues. With increased complexity of the model, it becomes harder to identity the sources of the convergence problems. For a proper model implementation, problems may also arise due to numerical and solver related issues. The lack of insight, or the knowledge required about the solution process, is one reason for that the identification is hard to make.

Finally, there is a variety of tutorials available from Comsol, which can help to gain information for the implementation. At the same time, it can be hard to combine and use the knowledge obtained from these tutorials in a good way for the modelling purpose of this work.

6.1   Convergence

The problems encountered with convergence are probably due to a combination of several factors. On an overall level, they involve the number of equations that should be solved and coupling between these, combined with a rather large number of defined parameters and variables. The model is sensitive to changes of several parameters and values set for the boundary conditions. This is especially apparent

as the model depends on specific parameter values to reach convergence. In order to change these parameter values more than approximately 10–20%, in principle the whole model implementation must be repeated which is very time consuming. Apart from problems obtained when increasing the complexity of the model, three main features have decreased the possibility of convergence

- High chemical reaction rates

- Gradient controlled mass transfer between different species

- Density changes of the gas

High chemical reaction rates, especially when coupled to the temperature via the Arrhenius expression, can cause the solution to oscillate and diverge. A remedy has been to carefully ramp up the reaction rates by conducting an auxiliary parameter sweep. An upper limit of the reaction rates have also been used. This, together with successively increasing the reaction rates, have been used extensively during the simulations. When convergence once has been reached, the reaction rate limit can often be removed.

Another method to improve convergence is to apply manual scaling of the concentrations [32]. When having magnitudes of the variables solved for that differ significantly, the solver might encounter problems. One reason for this is because the coefficient matrix, A, of the equation system $A\mathbf{x} = \mathbf{b}$ to be solved, becomes ill-conditioned. For a problem defined by an ill-conditioned coefficient matrix, small errors that arise during the computation can cause large errors in the final solution of the problem [33]. The scale factor in Comsol should be in the same order of magnitude as the expected value of the variable. By default, Comsol conducts the scaling automatically, which in general works well. Problems with the automatic scaling are generally encountered when the variable has a value close to zero, which is the case for species being consumed by a high reaction rate.

Compared to the bed, the reaction rates in the riser have been harder to implement without convergence problems. One reason may be that the species concentrations in general are low in this region, and in addition approach zero. When coupled to a reaction expression, low concentrations seem to amplify the convergence problems. The expression of the CO reaction has given some problems as well, the reason is the square root of the concentration of H_2O and O_2 in equation (3.14). In order for the solver to run well, the concentrations of H_2O and O_2 must be defined as strictly larger than zero since values very close to or less than zero give rise to errors from the solver. The concentrations have then been defined according to

$$C_{def} = max(C, \alpha), \tag{6.1}$$

where C is the real concentration and α is a number in the order of 10^{-15}. The concentrations defined according to equation (6.1) have been implemented in the rate expressions of the CO oxidation. This implies however a substantially increased

simulation time compared to if an expression without the square root is used.

The gradient controlled mass transfer, i.e., equation (3.4), gives especially rise to convergence problems when the gradient approaches zero. This is amplified by high values of the mass transfer coefficient, K_{be}, species with large concentrations and by the oxidation of H_2 and CO. When the CO and H_2 reactions are disabled, the range of values for K_{be} which gives converged solutions increases somewhat.

The coupling of the equations describing the mass transfer and the velocity of the gas seems to exacerbate the robustness of the model further. To overcome these problems the equations have, as a starting guess, been completely decoupled from each other. For example by setting a constant velocity in the species equations. Apart from this, all source terms, i.e. reactions and phase transitions, have been removed. If a converged solution is obtained, the couplings and the source terms are implemented step by step until the final setup is reached. However, when arriving at the fully coupled model, it is often very hard or impossible to re-make a change and obtain a converged solution. In order to do so, the whole procedure described must be repeated.

Although the robustness of the model in general is very low, it is more sensitive to changes in some parameters. Problems arise especially for lower values of the dispersion coefficients. One reason may be that the method used for the discretization is based on the Galerkin method, which can give instability in the solution for cases where the convective transport of the variable is dominating [32]. Stabilization methods for this kind of problems are provided in Comsol and have been tried but with no success. The method most extensively used for these types of problems has been to simplify the model enough until it converges and then build the model up again, step by step, as described above. Apart from what has been described, the mesh has been refined and different solvers have been tried when obtaining convergence problems but no improvements have been observed.

6.2 Implementation of the heat balance

The heat balance was implemented using the method described in Section 4.3. Convergence problems were however encountered when coupling the mass and the heat balance due to the temperature dependency of the reaction rates of H_2 and CO. A final result of the coupled mass and heat balance was obtained for the bottom bed only, with a constant temperature of $1123\,\mathrm{K}$ in the reaction rate expressions. The solution obtained does, however, suffer from the following shortcomings

- Heat leakage from the furnace through the primary air inlet

- Inconsistency in the global energy balance

One probable reason is that for this type of problem, the velocity must be coupled to both the temperature and the pressure when working with Comsol. The only

way of doing this seems to be to solve the momentum equations of the gas. This means a different modelling approach for both the mass and heat balance compared to what has been proposed in this work. The suggested interface to be used is the *Reacting Flow*, which solves the momentum equations together with the equations of the mass balance, for more information, see [29]. A further discussion of the suggested implementation is given in Chapter 7 and Appendix A.

7

Conclusions and prospects

7.1 Conclusions

In this work, a model describing the mass and heat transfer in a BFB boiler has been implemented in Comsol Multiphysics. The motion of the gas and the fuel are modelled using a semi-empirical approach, and the gas is divided into a bubble phase and an emulsion phase. Drying, devolatilisation and char combustion are included, as well as gas phase reactions.

The simplified approach used for the fluid dynamics could be implemented and coupled to the mass transfer, and the results obtained are reasonable. Problems with convergence were, however, encountered frequently, especially for high chemical reaction rates. The model obtained for the mass balance also lacks a desirable level of robustness and is very sensitive to changes of some parameter values.

The implementation of the heat balance seems to require solving the momentum equations of gas in order to not yield unreasonable results. Therefore, future work needs to re-define the model and the implementation in Comsol, both with regard to the mass transfer and the heat transfer.

The work also reveals that the high degree of freedom in Comsol requires a solid knowledge of how the problem is handled by the software. Else, there is a risk of obtaining unreasonable results and convergence problems, with little chance to understand the reasons.

7.2 Future work

Further work includes implementing the heat balance, and using another approach for obtaining the gas velocity. This means that the equations describing the mass transfer need to be reformulated. A possible set up is to replace all *Transport of Diluted Species* interfaces with one *Reacting Flow* interface. For the heat balance, the *Heat transfer in Fluids* interface is kept and is coupled to the *Reacting Flow* interface. If a converged and reasonable solution is obtained for this case, the next step could be to add another *Reacting Flow* interface. By doing so, the velocity field of both the bubble and the emulsion phase can be solved for. A further description of the suggested setup is given in Appendix A.

7. Conclusions and prospects

References

[1] U.S. Energy Information Administration. *International Energy Outlook 2013.*

[2] International Energy Agency. *Statistics.* Accessed: 2015-02-10. International Energy Agency. 2012. URL: http://www.iea.org/statistics/statisticssearch/report/?year=2012&country=WORLD&product=ElectricityandHeat.

[3] European Commission. *Communication from the commission to the European parliament and the council - Implementing the Energy Efficienct Directive - Commission Guidance.* 2014.

[4] European Climate Foundation. *Biomass for heat and power - Opportunity and economics.* 2010.

[5] Oka, S. N. *Fluidized Bed Combustion.* New York: Marcel Dekker, Inc.; 2004.

[6] Bañales-Lópezand, S., Norberg-Bohm, V. Public policy for energy technology innovation: A historical analysis of fluidized bed combustion development in the USA. *Energy Policy.* 2002;30:1173–1180.

[7] Leckner, B. *Developments in fluidized bed conversion during 2005 - 2010.* Gothenburg: Chalmers University of Technology; 2011.

[8] Jäntti, T., Räsänen, K. Circulating Fluidized Bed Technology towards 800MW$_e$ scale - Lagisza 460MW$_e$ Supercritical CFB Operation Experience. *Power Gen Europe 2011; Milan; Italy; 7 June through 9 June.*

[9] Myöhänen, K. *Modelling of combustion and sorbent reactions in three-dimensional flow environment of a circulating fluidized bed furnace.* PhD thesis. Lappeenranta: Lappeenranta University of Technology; 2011.

[10] Basu, P. *Combustion and Gasification in Fluidized Beds.* Boca Raton: CRC/Taylor & Francis; 2006.

[11] Leckner, B. Fluidized bed combustion: Mixing and pollutant limitation. *Progress in Energy and Combustion Science.* 1998;24(1):31–61.

[12] Grace, J. R., Leckner, B., Zhu, J., Cheng, Y. *Multiphase Flow Handbook.* Ed. by Crowe, C. T. Boca Raton: CRC Press; 2006. Chap. 5.

[13] Kunii, D., Levenspiel, O. *Fluidization Engineering.* 2nd ed. Newton, Massachusetts: Butterworth-Heinemann; 1991.

[14] Pallarès, D. *Fluidized bed combustion - modeling and mixing*. PhD thesis. Gothenburg: Chalmers University of Technology; 2008.

[15] Ratschow, L. *Three-Dimensional Simulation of Temperature Distributions in Large-Scale Circulating Fluidized Bed Combustors*. PhD thesis. Hamburg: Hamburg University of Technology - TUHH; 2009.

[16] Gómez-Barea, A., Leckner, B. Modeling of biomass gasification in fluidized bed. *Progress in Energy and Combustion Science*. 2010;36(4):444–509.

[17] Thunman, H. *Combustion Engineering*. Ed. by Thunman, H. Course material for MEN031. Gothenburg: Reproservice, Chalmers University of Technology; 2014. Chap. 9.

[18] Welty, J. R., Wicks, C. E., Wilson, R. E., Rorrer, G. L. *Fundamentals of Momentum, Heat, and Mass Transfer*. 5th ed. Hoboken: John Wiley & Sons, Inc.; 2008.

[19] Toomey, R. D., Johnstone, H. P. Gaseous fluidization of solid particles. *Chemical Engineering Progress*. 1952;48:220–226.

[20] Lundberg, L., Pallares, D., Johansson, R., Thunman, H. A 1-dimensional model of indirect biomass gasification in a dual fluidised bed system. *11th International Conference on Fluidized Bed Technology, CFB 2014; Beijing; China; 14 May 2014 through 17 May*. 2014:607–612.

[21] Ergun, S. Fluids flow through packed column. *Chemical Engineering Progress*. 1952;48(2):88–94.

[22] Wen, C. Y., Yu, Y. H. A generalized method for predicting the minimum fluidization velocity. *AIChE journal*. 1966;12(3):610–612.

[23] Sette, E. *Lateral mixing of solids in bubbling fluidized beds - experimental quantification*. PhD thesis. Gothenburg: Chalmers University of Technology; 2014.

[24] Olsson, J., Pallarès, D., Johnsson, F. Lateral fuel dispersion in a large-scale bubbling fluidized bed. *Chemical Engineering Science*. 2012;74:148–159.

[25] Niklasson, F., Thunman, H., Johnsson, F., Leckner, B. Estimation of Solids Mixing in a Fluidized-Bed Combustor. *Ind. Eng. Chem. Res.* 2002;41:4663–4673.

[26] Howard, J. B., Williams, G. C., Fine, D. Kinetics of carbon monoxide oxidation in postflame gases. *Symposium (International) on Combustion*. 1973;14(1):975–986.

[27] Di Blasi, C. Dynamic behaviour of stratified downdraft gasifiers. *Chemical Engineering Science*. 2000;55(15):2931–2944.

[28] Ranz, W. E. Friction and transfer coefficients for single particles and packed beds. *Chemical Engineering Progress*. 1952;48(5):247–253.

[29] Comsol. *Comsol Multiphysics Users Guide*. 2012.

[30] Liu, G., Quek, S. *The finite element method: a practical course.* Oxford; Boston: Butterworth-Heinemann; 2003.

[31] Thunman, H. *Combustion Engineering.* Ed. by Thunman, H. Course material for MEN031. Gothenburg: Reproservice, Chalmers University of Technology; 2014. Chap. Appendix B.

[32] Comsol. *Comsol Multiphysics Reference Guide.* 2012.

[33] Clay, D. C. *Linear Algebra and Its Applications.* 3rd ed. Boston: Pearson Addison - Wesley; 2006.

References

A
Additional information of the Comsol model

This chapter contains additional information about the model implementation in Comsol. Figure A.1 shows a screen shot of the model structure in Comsol.
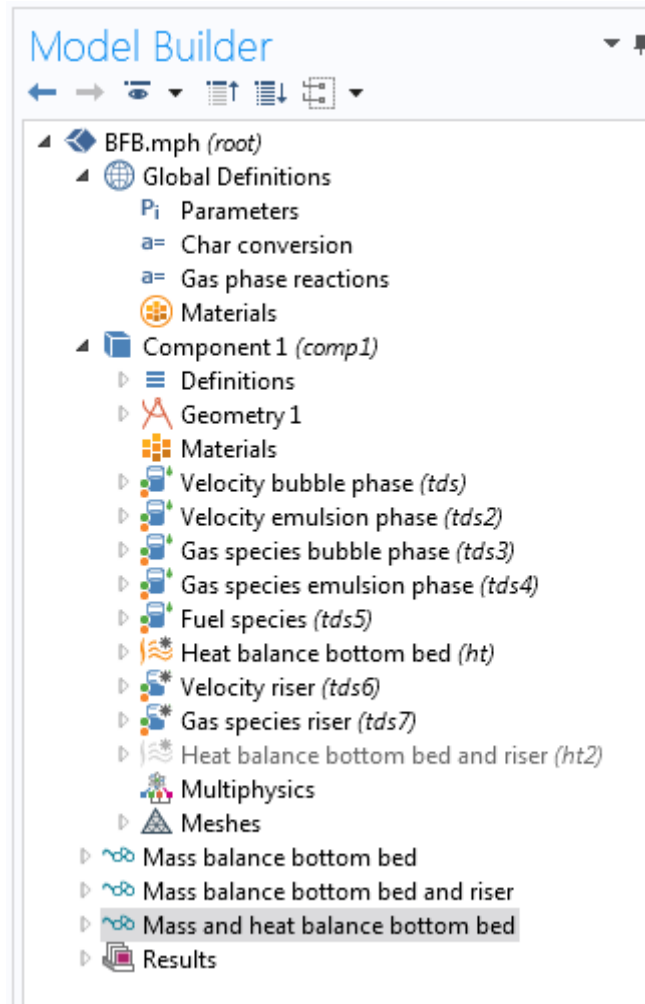

Figure A.1: *Model structure in Comsol. Under Component 1, below "Materials", the physics interfaces are located. The three studies defined are located below the "Meshes".*

The studies are as follows

- *Mass balance bottom bed*

- *Mass balance bottom bed and riser*

- *Mass and heat balance bottom bed*

All reaction rate expressions are defined for a constant temperature, T_init, defined as a parameter. Thus, when solving the heat balance, the chemical reaction rates are not coupled to the temperature. The reason is that convergence problems arise otherwise. The velocities that are defined in the interfaces *Gas species bubble phase*, *Gas species emulsion phase* and *Heat balance bottom bed* are however coupled to the variable temperature T.

A.1   Parameters

Under *Global definitions: Parameters*, all parameters are listed. The table includes the fuel composition and a calculation of the fuel's heating value in order to account for any modifications of the fuel composition, Chapter 4. Other features in the table are physical properties of the gas and the solids that are assumed to be constant, the molar fluxes of air and fuel, calculations of the fraction entering the bubble and the emulsion phase and the fraction of primary and secondary air. Note that if one wants to include the temperature dependence of the reaction rates, the last four parameters defined in the parameter table; k_Rg1, k_Rg2, D_O2_air and Sc_C need to be defined as variables that contain the temperature T.

There are several parameters named nu_xy_nk where xy=C or O2 and nk=12, 23, 34, 45. For index C, these are the stoichiometric coefficient of the char class $k+1$ that is produced when char class k is consumed. Indexes CO2 and O2 denote the corresponding coefficients for the O_2 and CO_2 consumed and produced. In the heat balance, the stoichiometric coefficients for O_2 are used. This is because the heat released for each class is given by the amount of char actually being combusted, which equals the molar consumption and generation of O_2 and CO_2, respectively.

A.2   Variables

Two tables containing variables are defined according to: *Global definitions; Char conversion* and *Global definitions; Gas phase reactions*. The first table contains calculations required for the char conversion, e.g. the Reynolds number for each char class. The reason for defining these as variables is to simplify the expressions implemented for the reaction rates in the source terms that account for the char conversion. The second table is defined for the CO and H_2 oxidation. Here, the concentration of CO and H_2O defined as larger than zero are found, together with the reaction rate expressions of the reactions. By keeping the latter as variables, it is easy to define limits on the reactions rates when convergence problems are encountered.

A.3 Geometry

The geometry is parametrized, i.e. the dimensions are defined as parameters. Three sections together constitute the furnace: *R1*, *R2* and *R3*; where *R1* is the domain of the bottom bed and *R2* and *R3* are those of the riser. Apart from these, the fuel inlet and the two secondary air inlets are defined and extruded. The reason for having rectangular, and not circular, fuel and secondary air inlets is to avoid a dense mesh at these inlets. The molar flow (i.e. the surface integration of the molar flux at the surfaces) is mesh dependent and when using circular inlets the risk of having a mesh that is too coarse to resolve the flow increases. This is probably because the representation of a circle is not being exact.

There have been some problems with running *Mass balance bottom bed* when the entire geometry is used. The segregated solver of the interface *Fuel species* has had problems with convergence. A remedy is to disable the geometry sections that define the riser, and try to run *Mass balance bottom bed* only for the geometry of the bottom bed. Why this problem is encountered is not understood. Thus, if running *Mass balance bottom bed* and convergence problems arise, it can be useful to try to run the simulation for the geometry of the bottom bed only.

A.4 Mesh

Under *Component 1; Meshes*, three meshes are defined. *Mesh 1* is a normal, physics controlled mesh which has been used in order to obtain efficient simulations when investigating different setups. *Mesh 2* and *Mesh 3* are refined at the interface connecting the bed and the riser. The reason for this is to obtain accurate molar flows from the bed to the riser. The difference between *Mesh 2* and *Mesh 3* is that the latter is finer.

A.5 Mass balance of the bottom bed

In the first study, *Mass balance bottom bed*, the mass balance of the bottom bed is solved. The simulation includes the five first interfaces under *Component 1*: *Velocity bubble phase*, *Velocity emulsion phase*, *Bubble phase species*, *Species emulsion phase* and *Fuel species*. Apart from defining the interfaces as conservative, no settings that differ from the default ones are present. The conservative setting is found in each interface, i.e. *Velocity bubble phase*, *Velocity emulsion phase*, *Bubble phase species*, *Species emulsion phase* and *Fuel species*, under *Advanced settings*.

In the study *Mass balance of the bottom bed; Step 1: Stationary*, there is an *Auxiliary sweep* defined for a parameter named k_ramp. The purpose of this parameter is to successively ramp up the reaction rate of CO and H_2. It is therefore multiplied with the reaction rates in the source terms *CO oxidation* and *H_2 oxidation* that are found in the interfaces *Velocity bubble phase*, *Velocity emulsion phase* and *Bubble phase species*.

A.6   Mass balance of the bottom bed and the riser

In the study *Mass balance bottom bed and riser; Step 1: Stationary* the solution from the mass balance of the bottom bed is used to define *Values of variables solved for* and *Values of variables not solved for.* An auxiliary sweep parameter k_ramp_riser is defined in the study, which ramps the reaction rates of the CO and H_2 reactions in the same way as described above.

In addition to the interfaces in *Mass balance bottom bed*, the study *Mass balance bottom bed and riser* includes the physics interfaces *Velocity riser* and *Gas species riser.* The molar fluxes of the species in the bubble and the emulsion phase are added in the boundary condition *Flux 1* of these two interfaces, respectively. Convergence problems can appear for this study, although no changes in the model have been made since the last time it was simulated. If this happens, a remedy is to run the *Mass balance bottom bed* study, and then try to run *Mass balance bottom bed and riser.* Why this problem is encountered is unclear.

A.7   Mass and heat balance of the bottom bed

In the study *Mass and heat balance of the bottom bed; Step 1: Stationary*, the solution from the mass balance of the bed is used for *Values of variables solved for* and *Values of variables not solved for.* The reason is to enhance convergence and speed up the simulation by providing Comsol good starting guesses. In addition to the physics interfaces solved for in the study *Mass balance bottom bed*, the physics interface *Heat balance bottom bed* is also included. Note that the unrealistic results from the heat balance of the bed especially can be seen in *Results; Derived values; Normal total energy flux in* and *Results; Normal total energy flux.*

The heat balance of the riser was not prioritized due to the unreasonable results obtained from the heat balance of the bed. Furthermore, in the late part of the work, convergence problems when running the coupled mass and heat balance for both the bed and the riser were encountered. The implementation is still present in the file, as a disabled physics interface *Heat transfer in riser.* In this interface, the heat balance of the bed and the riser is combined. In the disabled interface *Heat balance bottom bed and riser*, there are two sub tabs: *Heat Transfer in Fluids: Bed* and *Heat Transfer in Fluids: Riser.* The reason for having two of these is to account for that the gas velocities and the heat conductivity in the bed and the riser differs. Note that the scale factors k_ramp and k_ramp_riser are excluded in the expressions of the heat sources in this interface.

A.8 Suggestions for the implementation of the heat balance using *Reacting Flow*

For the *Reacting Flow* interface it possible to define whether it should be applied for turbulent or laminar flow. The total path for defining the interface is *Chemical Species Transport; Reacting Flow; Laminar Flow*. To couple the mass and heat transfer, a *Heat Transfer in Fluids* interface is also required. Available settings of the *Reacting Flow* interface are

- In *Reacting Flow*, under *Species*, select *Dilute Solution* or *Concentrated Species* to obtain a dilute or concentrated mass transfer

- Under *Fluids 1*, select ideal gas for the density and *Temperature (ht)* from the *Model inputs* (requires that you have added a *Heat Transfer in Fluids* interface)

The following settings for the boundary conditions can be selected

- Under *Inlet*, the inlet boundary condition can be defined as a mass flux or a velocity

- For the outlet boundary condition, *Outflow* can be selected

- Under *Wall*, the boundary condition of the walls can be defined by e.g. slip velocity or no slip

Under *Heat Transfer in Fluids; Heat Transfer Fluids 1*, the following settings are suggested

- In *Thermodynamics, Fluid*, select *Ideal gas* and *Mean Molar Mass* (by typing *rspf.Mn* in this field the mean molar mass is taken from the *Reacting Flow* interface.)

- In *Model inputs*, select *Pressure* from *Absolut Pressure (rspf)* and *Velocity Field* from *Velocity field (rspf/fluid1)*. The pressure and velocity is then taken from the *Reacting Flow* interface.

VI